Published in final edited form as:
Cardiovasc Toxicol. 2009 March ; 9(1): 30–38. doi:10.1007/s12012-009-9034-6.

Metabolites of MDMA induce oxidative stress and contractile dysfunction in adult rat left ventricular myocytes

Sylvia K. Shenouda[1], **Kurt J. Varner**[1,†], **Felix Carvalho**[2], and **Pamela A. Lucchesi**[3,†]

[1]Department of Pharmacology and Experimental Therapeutics, Louisiana State University Health Sciences Center, New Orleans, LA

[2]REQUIMTE, Department of Toxicology, Faculty of Pharmacy, University of Porto, Portugal

[3]Center for Cardiovascular and Pulmonary Research and the Heart Center, Nationwide Children's Hospital, Columbus, OH.

Abstract

Repeated administration of MDMA (ecstasy) produces eccentric left ventricular (LV) dilation and diastolic dysfunction. While the mechanism(s) underlying this toxicity are unknown; oxidative stress plays an important role. MDMA is metabolized into redox cycling metabolites that produce superoxide. In this study, we demonstrated that metabolites of MDMA induce oxidative stress and contractile dysfunction in adult rat left ventricular myocytes. Metabolites of MDMA used in this study included: alpha-methyl dopamine, N-methyl alpha-methyl dopamine and 2,5- bis(glutathion-S-yl)-alpha-MeDA. Dihydroethidium was used to detect drug-induced increases in reactive oxygen species (ROS) production in ventricular myocytes. Contractile function and changes in intracellular calcium transients were measured in paced (1Hz), Fura-2 AM loaded, myocytes using the IonOptix system. Production of ROS in ventricular myocytes treated with MDMA was not different from control. In contrast, all three metabolites of MDMA exhibited time- and concentration-dependent increases in ROS that were prevented by N-acetyl-cysteine (NAC). The metabolites of MDMA, but not MDMA alone, significantly decreased contractility and impaired relaxation in myocytes stimulated at 1Hz. These effects were prevented by NAC. Together, these data suggest that MDMA-induced oxidative stress in the left ventricle can be due, at least in part, to the metabolism of MDMA to redox active metabolites.

Keywords

ecstasy; rat; calcium; IonOptix

Introduction

MDMA (3,4-methylenedioxymethamphetamine), most commonly known by the street name ecstasy, is characterized as an amphetamine/stimulant, psychedelic (hallucinogen), or empathogenic-entactogen (1). Despite the popular misconception that ecstasy is "safe", MDMA can produce cardiac arrhythmias, myocardial infarction and dilated cardiomyopathy

†Corresponding Authors: Director, Center for Cardiovascular and Pulmonary Research The Research Institute at Nationwide Children's Hospital 700 Children's Drive Columbus, Ohio 43205. Tel: 614-722-4969 Fax: 614-722-4881 Pamela.lucchesi@nationwidechildrens.org Interim Head, Department of Pharmacology and Experimental Therapeutics Louisiana State University Health Sciences Center 1901 Perdido Street New Orleans, LA 70112 Tel: 504-568-4742 Fax: 504-568-2361 kvarne@lsuhsc.edu .

Conflict of interest: none declared

(2-5). We have previously shown that repeated binge administration of MDMA in rats produces myocarditis, accompanied with inflammatory infiltrates and areas of necrosis (6). Furthermore, binge administration of MDMA produces eccentric left ventricular dilation and diastolic dysfunction that is accompanied by cardiac myocyte contractile dysfunction and impaired relaxation (7). These structural and functional deficits were associated with enhanced left ventricular oxidative stress. The mechanism(s) by which MDMA produces oxidative stress in the heart remains to be determined.

It is widely reported that systemic administration of MDMA can damage central serotonergic neurons by an oxidative stress-dependent mechanism (8-10). Studies revealed that MDMA is metabolized to catechols that can undergo redox cycling, with the formation of reactive (and unstable) orthoquinones, generating large quantities of reactive oxygen and nitrogen species (11). The redox active metabolites of MDMA have also been implicated in the toxic effects of MDMA on the heart, kidney and liver (12-15) in vitro.

The effect of MDMA on isolated cardiac myocyte function has not been extensively studied. A report from Carvalho et al found that MDMA metabolites elicited cytotoxic effects on isolated cardiac myocytes including morphological changes and decreased activity of ROS scavenging systems (12). However, the effects of MDMA and its metabolites on cardiac myocyte excitation-contraction coupling are not known. Therefore, the first goal of this study was to determine whether MDMA and/or redox active metabolites of MDMA, alpha-methyl dopamine (α-MeDA), N-methyl alpha-methyl dopamine (N-Me-α-MeDA), or 2,5-bis(glutathion- S-yl)-alpha-MeDA (GSH-α-MeDA), increased oxidative stress in ALVM. The second goal of this study was to determine whether MDMA and/or metabolites of MDMA produce alterations in myocyte function by a ROS-dependent mechanism.

Materials and Methods

Materials

Liberase Blendzyme 4 (Roche), Laminin-Entactin free Mouse (BD Biosciences), Dihydroethidium (Sigma-Aldrich), Fura-2 AM (Invitrogen), N-acetyl cysteine (Sigma-Aldrich). MDMA was a gift from NIDA. Alpha-methyl dopamine (α-MeDA), 2,5-bis(glutathion- S-yl)-alpha-MeDA (GSH-α-MeDA) and N-methyl-alpha-methyl dopamine (N-Me-α-MeDA) were synthesized and purchased from Dr. Ana Lobo in the Organic Chemistry Department, Porto University (Portugal). A quantity of N-Me-α-MeDA was generously provided by Dr. David E. Nichols, Purdue University.

Male Sprague-Dawley rats (200-225 g; Harlan, Indianapolis, IN) were housed in a temperature- and humidity-controlled room with a 12-h light/dark cycle. Standard rat chow and tap water were available ad libitum. All procedures were performed in accordance with the National Institutes of Health Guidelines for the Care and Use of Experimental Animals and approved by the Institutional Animal Care and Use Committee at Louisiana State University Health Sciences Center.

Adult rat cardiac myocyte isolation

ALVM were enzymatically isolated as previously described (7). Briefly, rats were anesthetized with a mixture of ketamine and xylazine (100/10 mg/kg, i.p.), hearts were removed and retrogradely perfused via the aorta using perfusion buffer (Alliance for Cell Signaling, Protocol PP00000125) followed by digestion buffer (perfusion buffer containing 12.5 μM $CaCl_2$, 0.14 mg/ml trypsin and 0.25 mg/ml of Liberase Blendzyme 4. After digestion, the left ventricle was removed and minced in perfusion buffer with 12.5 μM $CaCl_2$ and 5% BSA. The concentration of $CaCl_2$ in the solution was gradually increased over 20 min to achieve a final concentration of 1 mM. ALVM were plated on 4-well culture

slides or Warner chambers (coated with laminin) in Minimal Essential Media (MEM) with Hanks' salts and 2 mM L-glutamine, supplemented with 5% calf serum, 10 mM 2,3-butanedione monoxime (BDM) and 100 U/ml penicillin. After 1 hr incubation, ALVM were rinsed and placed in culture medium (serum-free MEM with 0.1% BSA, 100 U/ml penicillin and 2 mM L-glutamine). Myocytes with obvious sarcolemmal blebs or spontaneous contractions were not used.

ALVM treatment

Freshly isolated ALVM were incubated in culture media for 1 hr, followed by a quick rinse using 1X PBS. The various drug and antioxidant treatments were added to the ALVM in serum-free MEM with 0.1% BSA, 100 U/ml penicillin and 2 mM L-glutamine and incubated for the desired treatment duration. In selected studies the antioxidant, N-acetyl cysteine (NAC), was added prior to treatment with MDMA or the metabolites of MDMA.

To measure concentration-dependent increases in ROS produced by MDMA or metabolite treatments, cells were plated on a 4-well chamber slide and incubated for 4 hrs with MDMA or the metabolites of MDMA (0.2, 0.4, or 0.6 mM). To measure time-dependent increases in ROS produced by MDMA and the metabolites of MDMA, cells were plated on 4 well chamber slides and MDMA or the metabolites of MDMA (0.4mM) were added to the cells for 1 min, 10 min, 20 min, 30 min, 1 hr, 2 hr or 4 hr.

Detection of ROS in ALVM

After 4hrs, the media was removed and fresh media containing 5 μM dihydroethidium (DHE) was added to the cells and incubated at 37°C with 95%O_2-5% CO_2 for 30 mins. In the presence of superoxide ($O^{\bullet -}_2$), hydrogen peroxide (H_2O_2), or hydroxyl radical ($OH^{\bullet}$), DHE is oxidized to ethidium, which intercalates into the nuclear DNA and can be visualized as a red nuclear pigment under ultraviolet light (excitation, 500-530 nm; emission, 590-620 nm). Cells were visualized using an inverted immunofluorescence microscope (Olympus, IX-70). Fluorescent images were obtained with a 10x objective using identical exposure times (2 s) and images were acquired using Slide Book software. DHE staining was quantified by calculating the percentage of DHE positive cells versus the total number of viable cells (detected by bright field exposure) in each of three separate fields (10X) per treatment (≈25 cells/field).

Contractility and intracellular Ca^{2+} in ALVM

The mechanical properties of ALVM were assessed using a SoftEdge video based edge-detection system (IonOptix Corporation, Milton, MA) as previously described (7). An n of 15 cells from at least three separate isolations was used for each group. Briefly, cells were incubated with Tyrode's buffer containing 1 μM Fura 2-AM (Molecular Probes) for 10 min and then washed with Tyrode's buffer to remove excess dye. Myocytes were field stimulated with suprathreshold voltage (20-25V) at 1 Hz (3-ms duration). Sarcomere length was monitored from a red-light bright-field image (650-nm long-pass filter) and sarcomere length was measured using an IonOptix MyoCam camera. For $[Ca^{2+}]_i$ imaging, Fura-2 AM-loaded ALVM were excited at 360±6.5 nm and 380±6.5 nm with an ultraviolet xenon lamp. Emission fluorescence was measured at 510±15 nm.

Contractility and changes in intracellular Ca^{2+} were analyzed using an IonWizard data acquisition system (IonOptix). For sarcomere shortening, absolute twitch amplitude was measured as the difference between the systolic and the diastolic sarcomere length; sarcomere length (SL) shortening % was expressed as the ratio of absolute twitch amplitude to diastolic sarcomere length. Shortening velocity (-dl/dt) was used to measure the maximum velocity of sarcomere shortening during contraction and relengthening velocity

(dl/dt) was used to assess the maximum velocity of sarcomere relengthening during relaxation. For the ratio of fluorescence intensities of Fura-2 AM (340nm/380nm), the amplitude was measured as the difference between baseline and peak length; Ca^{2+} transient amplitude was expressed as the ratio of absolute amplitude to transient baseline. Departure velocity was used to assess the maximum velocity of increase in intracellular Ca^{2+}. Return velocity was used to measure the maximum velocity of return of $[Ca^{2+}]_i$ to baseline.

Statistical Analysis

Data are reported as mean ± SEM. Statistical comparisons were made by one-way or two-way ANOVA, with the Bonferroni post hoc test (SigmaStat software) for group comparisons. Values of $P<0.05$ were considered statistically significant.

Results

Metabolites of MDMA increase ROS in a concentration-dependent manner

We used DHE staining to detect concentration-dependent increases in ROS using three different concentrations of MDMA (0.2, 0.4 and 0.6 mM), α-MeDA, N-Me-α-MeDA and GSH-α-MeDA (0.2, 0.4 and 0.6 mM). The 0.4 and 0.6 mM concentrations of α-MeDA and GSH-α-MeDA increased ROS in ALVM after 4 hrs of treatment as evidenced by the DHE stained nuclei (fig. 1B and 1D). All three concentrations of N-Me-α-MeDA increased ROS (fig. 1C). In contrast, MDMA failed to produce ROS in ALVM at any of the concentrations tested (fig. 1A).

Metabolites of MDMA increase ROS in a time-dependent manner

DHE staining was used to determine the time course of ROS production in ALVM treated with 0.4 mM of MDMA, N-Me-α-MeDA, α-MeDA or GSH-α-MeDA. DHE staining was evaluated at 1 min, 10 min, 20 min, 30 min, 1 hr, 2 hr and 4 hrs after drug treatment. ROS was significantly increased after 1, 2 and 4 hrs of treatment with α-MeDA or N-Me-α-MeDA (fig. 2). In ALVM treated with GSH-α-MeDA, significant increases in DHE staining were detected only after 2 hrs of treatment (fig. 2). In control and MDMA treated cells, there was no detectable DHE staining at any of the time points tested (fig. 2).

N-acetyl cysteine prevents ROS elevation induced by metabolites of MDMA

We used N-acetyl cysteine (NAC), a glutathione precursor, to prevent metabolite-induced increases in ROS production in ALVM. ALVM were treated with MDMA (0.4 mM) or the metabolites of MDMA (0.4 mM) with or without NAC (1 mM) for 4 hrs. Compared to control, α-MeDA, GSH-α-MeDA and N-Me-α-MeDA significantly increased DHE staining (fig. 3). Co-treatment with NAC significantly reduced ROS production elicited by α-MeDA, GSH-α-MeDA or N-Me-α-MeDA (fig. 3). As before, treatment with MDMA failed to increase ROS in ALVM (fig. 3). Cells treated with NAC or MDMA plus NAC did not show any statistically significant increase in ROS production (data not shown).

Metabolites of MDMA induce contractile dysfunction in ALVM

To test whether metabolite-mediated increases in ROS were associated with mechanical dysfunction and/or impaired $[Ca^{2+}]_i$ handling, we compared contractile function (1 Hz stimulation) and changes in $[Ca^{2+}]_i$ (using Fura-2 AM) in ALVM treated with MDMA, α-MeDA, N-Me-α-MeDA or GSH-α-MeDA alone and in combination with NAC (1 mM).

Compared to control ALVM, the contractile responses (measured by SL shortening %) in ALVM treated with α-MeDA or GSH-α-MeDA were significantly decreased, while contractility was not affected by treatment with MDMA or N-Me-α-MeDA (fig. 4A). Co-

treatment with NAC prevented or attenuated the decrease in contractility produced by α-MeDA and GSH-α-MeDA, respectively (fig. 4A). The amplitude of the intracellular Ca^{2+} transient in these cells was not affected by any of the treatments with or without NAC (fig. 4B).

We next determined the kinetics of the contractile responses and the intracellular Ca^{2+} transients in ALVM treated with MDMA or its metabolites. α-MeDA or GSH-α-MeDA significantly decreased –dl/dt (maximum velocity of shortening) compared to controls; however, –dl/dt was not significantly different in ALVM treated with MDMA or N-Me-α-MeDA (fig. 4C). The velocity of Ca^{2+} release from intracellular stores (departure velocity) was unchanged by treatment with MDMA, α-MeDA or GSH-α-MeDA compared to control (fig. 4D). Interestingly, ALVM treated with N-Me-α-MeDA exhibited a significant increase in departure velocity of Ca^{2+} (fig. 4D). The decrease in –dl/dt produced by α-MeDA was prevented by NAC. NAC only partially prevented the decrease in –dl/dt produced by GSH-α-MeDA and had no effect on the response elicited by MDMA or N-Me-α-MeDA (fig. 4C). Co-administration of NAC did not affect intracellular Ca^{2+} departure velocity in any of the groups tested (fig. 4D).

The maximum velocity of relengthening (dl/dt, relaxation velocity), was significantly decreased in cells treated with GSH-α-MeDA compared to control ALVM (fig. 4E); this effect was attenuated by co-treatment with NAC (fig. 4E). MDMA, N-Me-α-MeDA, or α-MeDA had no significant effect on dl/dt compared to untreated controls (fig. 4E).

Ca^{2+} return velocity, a measure of the rate of intracellular Ca^{2+} uptake, was significantly increased by treatment with N-Me-α-MeDA (fig. 4F). This increase in return velocity was not affected by co-treatment with NAC (1 mM) (fig. 4F). In contrast, treatment with GSH-α-MeDA decreased the return velocity of intracellular Ca^{2+}, which was prevented by co-treatment with NAC (fig. 4F). There was no change in intracellular Ca^{2+} return velocity in ALVM treated with MDMA or α-MeDA (fig. 4F), and co-treatment with NAC did not affect these responses.

Discussion

Despite the popular misconception that MDMA is “safe”, MDMA produces a number of actions on the cardiovascular system similar to other sympathomimetic stimulants (2,3,16-20). We have previously shown that rat hearts subjected to four MDMA binges exhibit myocarditis with inflammatory infiltrates and areas of necrosis, eccentric left ventricular dilation and diastolic dysfunction (6,7). While the mechanism(s) responsible for MDMA-mediated left ventricular dysfunction is unknown, our data show that oxidative stress may play an important role (7). Nonetheless, the question of how MDMA produces oxidative stress in the heart remains unanswered. Potential mechanisms include catecholaminergic stimulation or autooxidation of catecholamines (21), mitochondrial dysfunction and leukocyte recruitment and activation (6), and or coronary vasospasm-induced reperfusion ischemia (6,21). Recent studies have shown that MDMA metabolites play an important role in the toxicity of this drug (12-15). For example, MDMA is metabolized to catechols, which subsequently form orthoquinones. Orthoquinones are highly redox active molecules that can undergo redox cycling to generate reactive oxygen and nitrogen species (11). This raises the possibility that redox active metabolites of MDMA play a role in MDMA-induced oxidative stress in the heart.

As is the case with all in vitro pharmacological studies, there are questions regarding the relevance of the drug concentrations used, compared to those attained in humans. In short-term mechanistic studies of toxicity, the use of concentrations sufficient to provide

measurable, unambiguous effects is a common and mandatory practice. Our test concentrations of MDMA and its metabolites were determined after determining dose-response relationships. In addition, Rafael de la Torre and colleagues (22) showed that administration of 100 mg of MDMA (typical content of one tablet) in human volunteers produced maximum plasma concentrations of MDMA and N-Me-α-MeDA of 222.5±26.1 and 154.5±76.6 μg/L, roughly corresponding to 1 μM of each. Nevertheless, experienced ecstasy users are known to take as many as 8 tablets per session (23), which would result in much higher plasma concentrations of MDMA and its metabolites. In one report, the antemortem serum concentration of MDMA in a young female who took 12 ecstasy tablets was about 20 μM, while the postmortem MDMA concentrations in blood taken from the heart were about 138 μM (24). While postmortem redistribution may contribute to the high MDMA concentration in the heart, this concentration is similar to that tested in the present study.

Our data provide the first demonstration that MDMA metabolites can increase the production of ROS in ALVM, in a time- and concentration-dependent manner. In contrast, MDMA itself did not increase ROS production in ALVM, supporting other data that MDMA does not produce morphological or toxic effects in ALVM (12). MDMA is demethylated in the liver by CYP2D6, although other isoforms (CYP1A2, CYP2B6 and CYP3A4) may also contribute to the total oxidative metabolism of the drug (Carmo et al, 2006). The extrahepatic distribution of these P450 enzymes suggests that little if any MDMA is metabolized in the heart (Pavek and Dvorak, 2008).

While the mechanisms are unknown, most evidence indicates that the metabolites of MDMA transit to and enter cardiac cells. N-Me-α-MeDA and α-MeDA can then be oxidized by catecholamine metabolizing enzymes to their corresponding intermediate ortho-quinones, which then enter redox cycles to their semiquinone radicals leading to ROS production. The ortho-quinones can then cyclize, forming toxic aminochromes (11). In addition, the othro-quinones can be conjugated with GSH to form 5-(glutathion-S-yl)-α-MeDA and 5-(glutathion-S-yl)- N-Me-α-MeDA, respectively (25) which can be readily oxidized to the quinone-thioethers generating ROS (26). The conjugation of GSH with these metabolites can further increase intracellular ROS by depleting this important antioxidant defense mechanism. N-Me-α-MeDA and α-MeDA also decreased the activity of the antioxidant enzymes glutathione reductase, glutathione peroxidase and glutathione-S-transferase in ALVM (12).

To test whether an antioxidant could prevent increased ROS production in myocytes treated with metabolites of MDMA, we co-treated ALVM with N-acetyl cysteine (NAC) and the metabolites of MDMA. NAC provides an alternate means of raising intracellular glutathione (GSH, L-gamma-glutamyl-L-cysteinylglycine) via elevating intracellular cysteine or acting directly as a strong antioxidant. Furthermore, metabolites of MDMA are known to conjugate with intracellular GSH leading to GSH depletion, without a corresponding increase in GSSG, which may render the cells more susceptible to the effects of increased ROS. Our results show that the increases in ROS in ALVM treated with N-Me-α-MeDA, α-MeDA, or GSH-α-MeDA were blocked by NAC. This conclusion is in agreement with other studies that showed that either antioxidants or the overexpression of superoxide dismutase (SOD) in transgenic mice prevent MDMA-induced neurotoxicity in rats and mice (9,10,27-30). Furthermore, in freshly isolated rat hepatocytes, pretreatment with ascorbic acid or NAC prevents GSH depletion, decreases in ATP levels, loss of cell viability and the decrease in antioxidant enzymes activities produced by treatment with N-Me-α-MeDA (14).

In summary, our data show that MDMA is not capable of increasing ROS levels in ALVM, while metabolites of MDMA significantly increased ROS levels in a time-and

concentration-dependent manner. The increase in ROS was prevented by co-treatment with NAC.

Increases in ROS decrease myocyte contractile function in a concentration-dependent manner (31,32). Our data reveal for the first time that the increase in ROS produced by MDMA metabolites are associated with decreased contractility and impaired relaxation in ALVM. Treatment with α-MeDA or GSH-α-MeDA significantly decreased contractility (decreased sarcomere length shortening and -dl/dt). Contractility was also significantly decreased in ALVM isolated from rats subjected to four MDMA binges (7). Surprisingly, the decreases in contractility were not associated with changes in the Ca^{2+} transient amplitude, or decreases in velocity of Ca^{2+} release from intracellular stores. How these metabolites decreased contractility, without changing intracellular Ca^{2+}, is unknown; however, increased ROS have been shown to decrease the sensitivity of the myofilament to changes in intracellular Ca^{2+} (33). Furthermore, ROS can produce contractile dysfunction by inducing ASK1-dependent phosphorylation of cardiac troponin-T (cTn-T) (34) and activation of p90 Ribosomal S6 Kinase (p90RSK), which phosphorylates cardiac troponin I decreasing cTn-I Ca^{2+} sensitivity (35). The decreases in contractility and DHE fluorescence were prevented with treatment of α-MeDA, and significantly reduced in cells treated with GSH-α-MeDA by NAC, indicating that metabolite-mediated increases in ROS play an important role in the contractile deficits. In addition to producing contractile deficits, GSH-α-MeDA also significantly impaired relaxation (decreased dl/dt) in ALVM. This finding is consistent with our data showing that binge administration of MDMA in vivo produces diastolic dysfunction (7).

Contractile dysfunction produced in ALVM by MDMA metabolites may also reflect a decrease in intracellular ATP levels. α-MeDA and N-Me-α-MeDA or their oxidation products decrease ATP levels in ALVM and hepatocytes (12,14). Aminochromes, which are formed by the oxidation of MDMA metabolites, also decrease mitochondrial ATP production (36,37). Furthermore, ROS can directly inhibit protein complexes in the mitochondrial electron transport chain, decreasing ATP production (38-41). We have shown that MDMA treatment in vivo increases oxidative stress in the heart and causes the nitration of complexes III and V in the mitochondrial electron transport chain (7).

Contractility and relaxation were not decreased in ALVM treated with N-Me-α-MeDA, in spite of the fact that this metabolite increased ROS production in ALVM. There was a trend towards an increase in the amplitude of intracellular Ca^{2+} after treatment with this metabolite; however, this increase was not statistically significant. This metabolite did significantly increase the velocity of Ca^{2+} release and Ca^{2+}reuptake; whether either of these factors could overcome a decrease in myofilament Ca^{2+}sensitivity is not known and is the subject of future investigations. The observed increase in the velocity of Ca^{2+} release may reflect the oxidation of N-Me-α-MeDA resulting in the formation of N-Me-α-MeDA quinone, which increases the release of Ca^{2+} from intracellular stores and inhibits Ca^{2+} efflux from the cell (42). Furthermore, ROS can increase the opening probability of ryanodine receptors, decrease uptake of $Ca^{2+}$by SERCA, and enhance Na^{+}/Ca^{2+} exchanger-mediated Ca^{2+} fluxes, all of which would affect Ca^{2+} homeostasis in the myocardium (43).

In summary, metabolites of MDMA (α-MeDA, N-Me-α-MeDA and GSH-α-MeDA) produced concentration-related increases in ROS in ALVM. α-MeDA and GSH-α-MeDA, but not N-Me- α-MeDA, decreased ALVM contractility without changing intracellular Ca^{2+} transients. MDMA alone did not increase ROS production or alter contractile function. The contractile dysfunction produced by α-MeDA and GSH-α-MeDA was prevented or attenuated, respectively, by antioxidant treatment with NAC, suggesting that metabolite-induced decreases in ALVM contractility are mediated by increased ROS production. These

data suggest that redox active metabolites of MDMA play a substantial role in mediating the previously reported cardiotoxic actions of this drug.

Acknowledgments

We thank Ana Lobo (REQUIMTE/CQFB, Chemistry Department, Faculty of Science and Technology, New University of Libson, Portugal) for the synthesis of MDMA metabolites, Dr. David E. Nichols (Purdue University) for providing a quantity of N-Me-α-MeDA and NIDA for generously providing us with MDMA.

Funding. This work was supported by the American Heart Association Predoctoral Fellowship (615646, SKS), American Heart Association Grant-in-Aid (655796, KJV). National Institutes of Health RO1 HL63318-05 (PAL) and NCRR P20RR18766 (KJV, PAL).

References

1. Nichols DE. Differences between the mechanism of action of MDMA, MBDB, and the classic hallucinogens. Identification of a new therapeutic class: entactogens. J Psychoactive Drugs 1986;18:305–313. [PubMed: 2880944]
2. Lai TI, Hwang JJ, Fang CC, Chen WJ. Methylene 3, 4 dioxymethamphetamine-induced acute myocardial infarction. Ann Emerg Med 2003;42:759–762. [PubMed: 14634599]
3. Madhok A, Boxer R, Chowdhury D. Atrial fibrillation in an adolescent--the agony of ecstasy. Pediatr Emerg Care 2003;19:348–349. [PubMed: 14578836]
4. Sadeghian S, Darvish S, Shahbazi S, Mahmoodian M. Two ecstasy-induced myocardial infarctions during a three month period in a young man. Arch Iran Med 2007;10:409–412. [PubMed: 17604486]
5. Mizia-Stec K, Gasior Z, Wojnicz R, Haberka M, Mielczarek M, Wierzbicki A, Pstras K, Hartleb M. Severe dilated cardiomyopathy as a consequence of Ecstasy intake. Cardiovasc Pathol 2008;17:250–253. [PubMed: 18402796]
6. Badon LA, Hicks A, Lord K, Ogden BA, Meleg-Smith S, Varner KJ. Changes in cardiovascular responsiveness and cardiotoxicity elicited during binge administration of Ecstasy. J Pharmacol Exp Ther 2002;302:898–907. [PubMed: 12183645]
7. Shenouda SK, Lord KC, McIlwain E, Lucchesi PA, Varner KJ. Ecstasy produces left ventricular dysfunction and oxidative stress in rats. Cardiovasc Res 2008;79:662–670. [PubMed: 18495670]
8. Sprague JE, Nichols DE. The monoamine oxidase-B inhibitor L-deprenyl protects against 3,4-methylenedioxymethamphetamine-induced lipid peroxidation and long-term serotonergic deficits. J Pharmacol Exp Ther 1995;273:667–673. [PubMed: 7538579]
9. Colado MI, O'Shea E, Granados R, Murray TK, Green AR. In vivo evidence for free radical involvement in the degeneration of rat brain 5-HT following administration of MDMA ('ecstasy') and p-chloroamphetamine but not the degeneration following fenfluramine. Br J Pharmacol 1997;121:889–900. [PubMed: 9222545]
10. Colado MI, Green AR. The spin trap reagent alpha-phenyl-N-tert-butyl nitrone prevents 'ecstasy'-induced neurodegeneration of 5-hydroxytryptamine neurones. Eur J Pharmacol 1995;280:343–346. [PubMed: 8566105]
11. Bolton JL, Trush MA, Penning TM, Dryhurst G, Monks TJ. Role of quinones in toxicology. Chem Res Toxicol 2000;13:135–160. [PubMed: 10725110]
12. Carvalho M, Remiao F, Milhazes N, Borges F, Fernandes E, Mdo C. Monteiro, Goncalves MJ, Seabra V, Amado F, Carvalho F, Bastos ML. Metabolism is required for the expression of ecstasy-induced cardiotoxicity in vitro. Chem Res Toxicol 2004;17:623–632. [PubMed: 15144219]
13. Carvalho M, Hawksworth G, Milhazes N, Borges F, Monks TJ, Fernandes E, Carvalho F, Bastos ML. Role of metabolites in MDMA (ecstasy)-induced nephrotoxicity: an in vitro study using rat and human renal proximal tubular cells. Arch Toxicol 2002;76:581–588. [PubMed: 12373454]
14. Carvalho M, Remiao F, Milhazes N, Borges F, Fernandes E, Carvalho F, Bastos ML. The toxicity of N-methyl-alpha-methyldopamine to freshly isolated rat hepatocytes is prevented by ascorbic acid and N-acetylcysteine. Toxicology 2004;200:193–203. [PubMed: 15212815]

15. Ninkovic M, Malicevic Z, Selakovic V, Simic I, Vasiljevic I. N-methyl-3,4-methylenedioxyamphetamine-induced hepatotoxicity in rats: oxidative stress after acute and chronic administration. Vojnosanit Pregl 2004;61:125–131. [PubMed: 15296116]
16. Schifano F, Oyefeso A, Webb L, Pollard M, Corkery J, Ghodse AH. Review of deaths related to taking ecstasy, England and Wales, 1997-2000. BMJ 2003;326:80–81. [PubMed: 12521971]
17. Milroy CM, Clark JC, Forrest AR. Pathology of deaths associated with “ecstasy” and “eve” misuse. J Clin Pathol 1996;49:149–153. [PubMed: 8655682]
18. Duflou J, Mark A. Aortic dissection after ingestion of “ecstasy” (MDMA). Am J Forensic Med Pathol 2000;21:261–263. [PubMed: 10990289]
19. Henry JA, Jeffreys KJ, Dawling S. Toxicity and deaths from 3,4-methylenedioxymethamphetamine (“ecstasy”). Lancet 1992;340:384–387. [PubMed: 1353554]
20. Qasim A, Townend J, Davies MK. Ecstasy induced acute myocardial infarction. Heart 2001;85:E10. [PubMed: 11359764]
21. Jiang JP, Downing SE. Catecholamine cardiomyopathy: review and analysis of pathogenetic mechanisms. Yale J Biol Med 1990;63:581–591. [PubMed: 2092415]
22. de la Torre R, Farre M, Roset PN, Pizarro N, Abanades S, Segura M, Segura J, Cami J. Human pharmacology of MDMA: pharmacokinetics, metabolism, and disposition. Ther Drug Monit 2004;26:137–144. [PubMed: 15228154]
23. Verheyden SL, Henry JA, Curran HV. Acute, sub-acute and long-term subjective consequences of ‘ecstasy’ (MDMA) consumption in 430 regular users. Hum Psychopharmacol 2003;18:507–517. [PubMed: 14533132]
24. Elliott SP. MDMA and MDA concentrations in antemortem and postmortem specimens in fatalities following hospital admission. J Anal Toxicol 2005;29:296–300. [PubMed: 16105252]
25. Hiramatsu M, Kumagai Y, Unger SE, Cho AK. Metabolism of methylenedioxymethamphetamine: formation of dihydroxymethamphetamine and a quinone identified as its glutathione adduct. J Pharmacol Exp Ther 1990;254:521–527. [PubMed: 1974641]
26. Miller RT, Lau SS, Monks TJ. 2,5-Bis-(glutathion-S-yl)-alpha-methyldopamine, a putative metabolite of (+/−)-3,4-methylenedioxyamphetamine, decreases brain serotonin concentrations. Eur J Pharmacol 1997;323:173–180. [PubMed: 9128836]
27. Yeh SY. N-tert-butyl-alpha-phenylnitrone protects against 3,4-methylenedioxymethamphetamine-induced depletion of serotonin in rats. Synapse 1999;31:169–177. [PubMed: 10029234]
28. Gudelsky GA. Effect of ascorbate and cysteine on the 3,4-methylenedioxymethamphetamine-induced depletion of brain serotonin. J Neural Transm 1996;103:1397–1404. [PubMed: 9029406]
29. Aguirre N, Barrionuevo M, Ramirez MJ, Del Rio J, Lasheras B. Alpha-lipoic acid prevents 3,4-methylenedioxy-methamphetamine (MDMA)-induced neurotoxicity. Neuroreport 1999;10:3675–3680. [PubMed: 10619665]
30. Cadet JL, Ladenheim B, Baum I, Carlson E, Epstein C. CuZn-superoxide dismutase (CuZnSOD) transgenic mice show resistance to the lethal effects of methylenedioxyamphetamine (MDA) and of methylenedioxymethamphetamine (MDMA). Brain Res 1994;655:259–262. [PubMed: 7812784]
31. Sabri A, Byron KL, Samarel AM, Bell J, Lucchesi PA. Hydrogen peroxide activates mitogen-activated protein kinases and Na+-H+ exchange in neonatal rat cardiac myocytes. Circ Res 1998;82:1053–1062. [PubMed: 9622158]
32. Kwon SH, Pimentel DR, Remondino A, Sawyer DB, Colucci WS. H(2)O(2) regulates cardiac myocyte phenotype via concentration-dependent activation of distinct kinase pathways. J Mol Cell Cardiol 2003;35:615–621. [PubMed: 12788379]
33. Gao WD, Liu Y, Marban E. Selective effects of oxygen free radicals on excitation-contraction coupling in ventricular muscle. Implications for the mechanism of stunned myocardium. Circulation 1996;94:2597–2604. [PubMed: 8921806]
34. He X, Liu Y, Sharma V, Dirksen RT, Waugh R, Sheu SS, Min W. ASK1 associates with troponin T and induces troponin T phosphorylation and contractile dysfunction in cardiomyocytes. Am J Pathol 2003;163:243–251. [PubMed: 12819028]
35. Itoh S, Ding B, Bains CP, Wang N, Takeishi Y, Jalili T, King GL, Walsh RA, Yan C, Abe J. Role of p90 ribosomal S6 kinase (p90RSK) in reactive oxygen species and protein kinase C beta (PKC-

beta)-mediated cardiac troponin I phosphorylation. J Biol Chem 2005;280:24135–24142. [PubMed: 15840586]

36. Bindoli A, Rigobello MP, Galzigna L. Toxicity of aminochromes. Toxicol Lett 1989;48:3–20. [PubMed: 2665188]
37. Taam GM, Takeo S, Ziegelhoffer A, Singal PK, Beamish RE, Dhalla NS. Effect of adrenochrome on adenine nucleotides and mitochondrial oxidative phosphorylation in rat heart. Can J Cardiol 1986;2:88–93. [PubMed: 3635424]
38. Pearce LL, Kanai AJ, Epperly MW, Peterson J. Nitrosative stress results in irreversible inhibition of purified mitochondrial complexes I and III without modification of cofactors. Nitric Oxide 2005;13:254–263. [PubMed: 16185902]
39. Guidarelli A, Fiorani M, Cantoni O. Enhancing effects of intracellular ascorbic acid on peroxynitrite-induced U937 cell death are mediated by mitochondrial events resulting in enhanced sensitivity to peroxynitrite-dependent inhibition of complex III and formation of hydrogen peroxide. Biochem J 2004;378:959–966. [PubMed: 14627438]
40. Cassina A, Radi R. Differential inhibitory action of nitric oxide and peroxynitrite on mitochondrial electron transport. Arch Biochem Biophys 1996;328:309–316. [PubMed: 8645009]
41. Radi R, Cassina A, Hodara R, Quijano C, Castro L. Peroxynitrite reactions and formation in mitochondria. Free Radic Biol Med 2002;33:1451–1464. [PubMed: 12446202]
42. Orrenius S, McConkey DJ, Bellomo G, Nicotera P. Role of Ca2+ in toxic cell killing. Trends Pharmacol Sci 1989;10:281–285. [PubMed: 2672472]
43. Zima AV, Blatter LA. Redox regulation of cardiac calcium channels and transporters. Cardiovasc Res 2006;71:310–321. [PubMed: 16581043]

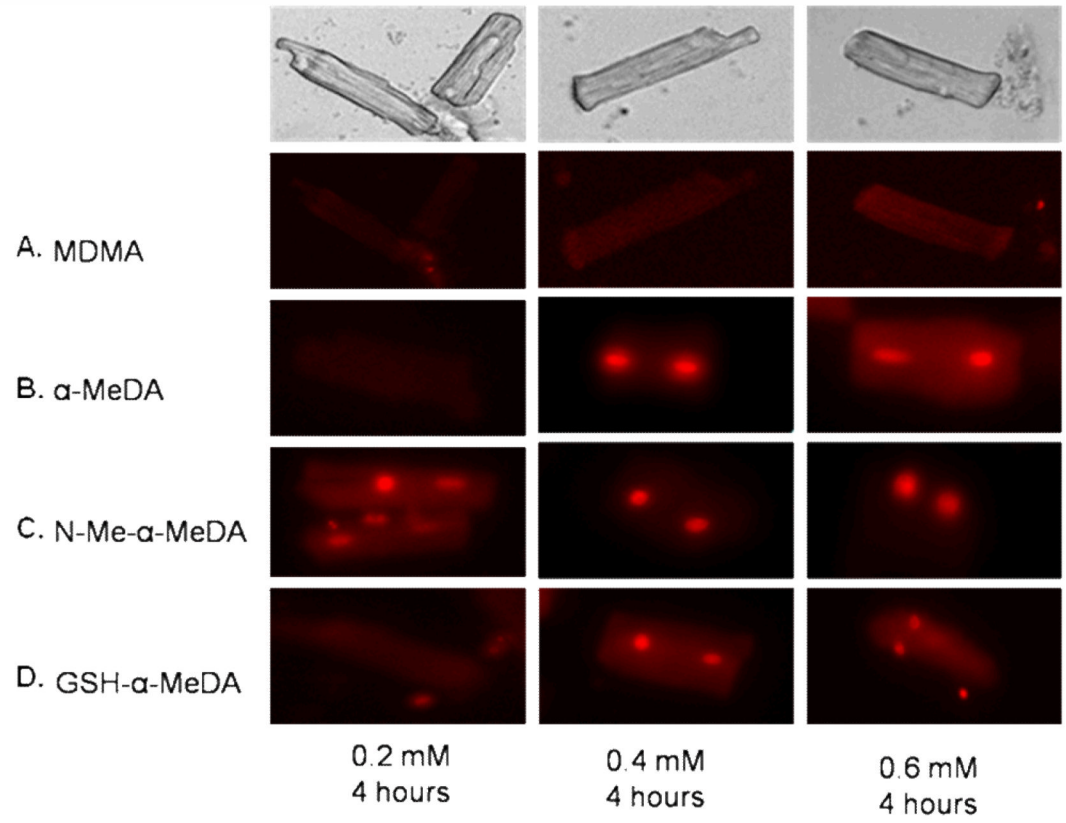

Figure. 1.

Dihydroethidium (DHE) staining of ALVM in response to treatment with MDMA or the metabolites of MDMA (alpha Methyl Dopamine (α-MeDA), N-Methyl-alpha-Methyl Dopamine (N-Me-α-MeDA), and glutathione alpha Methyl Dopamine (GSH-α-MeDA)). Nuclear staining denotes the presence of ROS. A: 0.2, 0.4, and 0.6 mM MDMA. B: 0.2, 0.4, and 0.6 mM α-MeDA. C: 0.2, 0.4, and 0.6 mM N-Me-α-MeDA, and D: 0.2, 0.4, and 0.6 mM GSH-α-MeDA.

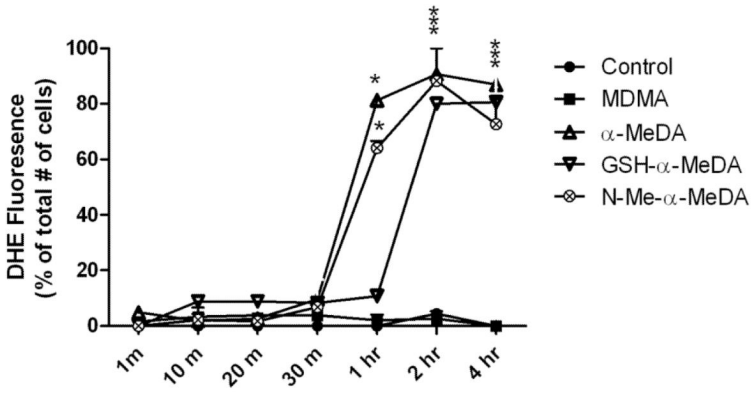

Figure. 2.

Summary of the time-course of DHE staining in ALVM treated with 0.4 mM MDMA or MDMA metabolites at 1min, 10 min, 20 min, 30 min, 1 hr, 2 hr, and 4 hr. Data presented as % of DHE positive cells/well at each time point, three fields/well were counted. * $p<0.05$ versus control.

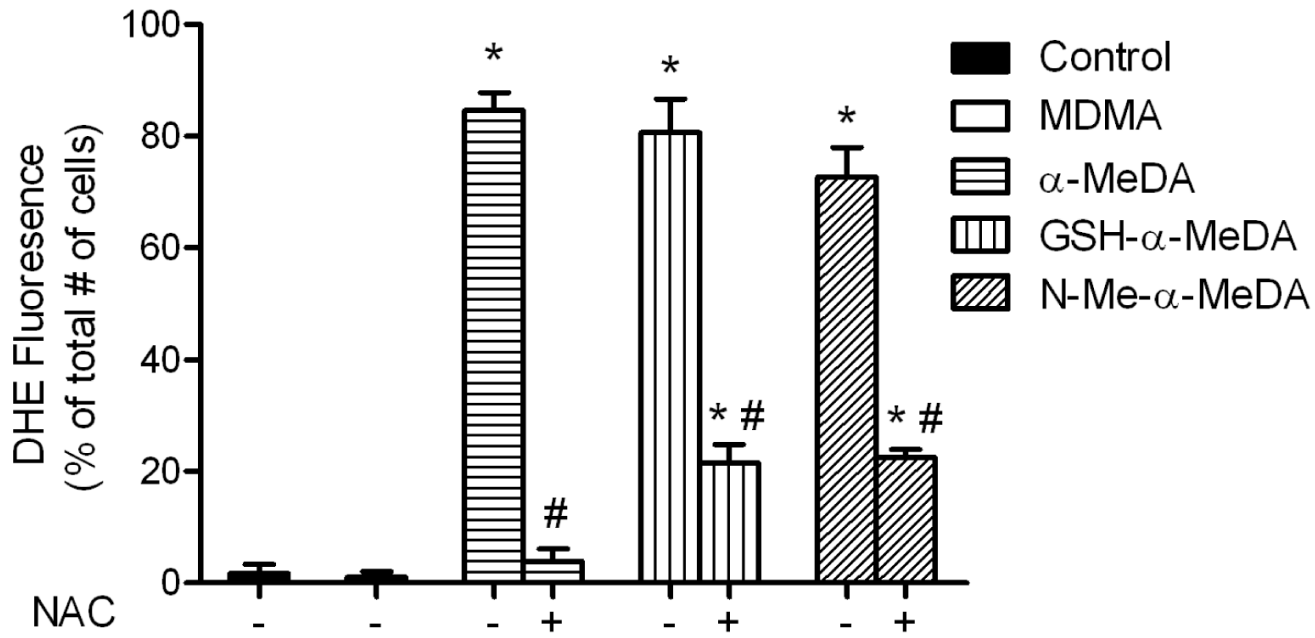

Figure. 3.

Effects of NAC on ROS production in ALVM treated with metabolites of MDMA. DHE staining of ALVM exposed to MDMA (0.4 mM), α-MeDA (0.4 mM), α-MeDA+NAC (0.4mM +1mM), GSH-α-MeDA (0.4 mM), GSH-α-MeDA+NAC (0.4mM +1mM), N-Me-α-MeDA (0.4 mM), or N-Me-α-MeDA+NAC (0.4mM +1mM) for 4 hours. *p<0.05 versus control. # p<0.05 versus treatment.

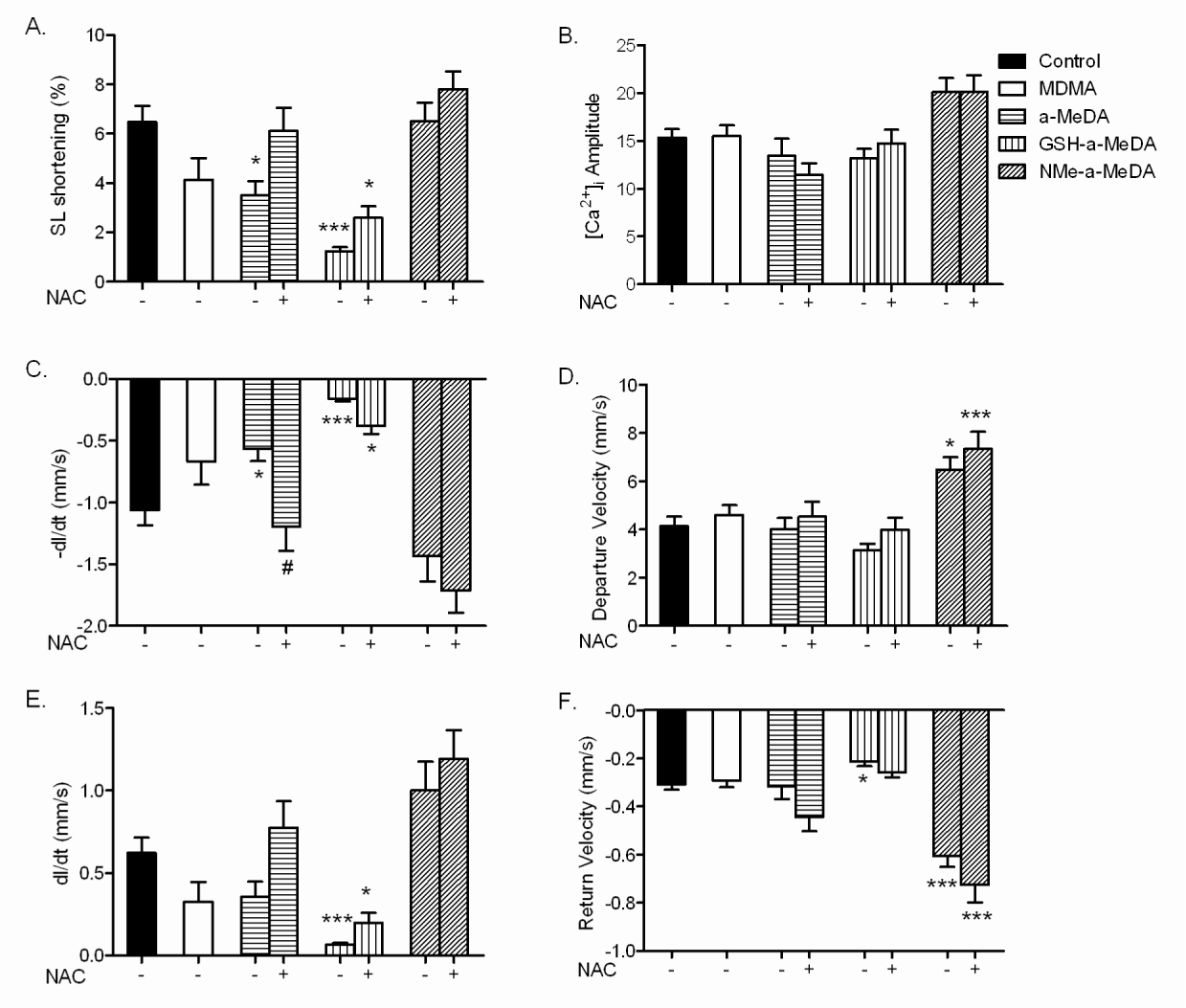

Figure. 4.

Effects of MDMA and its metabolites on ALVM contractility and intracellular Ca^{2+} handling during stimulated (1 Hz) contraction of Fura-2 AM loaded ALVM. A: Sarcomeric length shortening (SL shortening %). B: Amplitude of Ca^{2+} transient. C: Maximum velocity of shortening (–dl/dt). D: Maximum velocity of Ca^{2+} release as measured by departure velocity. E: Maximum velocity of relengthening (dl/dt). F: Maximum velocity of intracellular Ca^{2+} reuptake as measured by return velocity. ALVM exposed to MDMA (0.4 mM), α-MeDA (0.4 mM), α-MeDA+NAC (0.4mM +1mM), GSH-α-MeDA (0.4 mM), GSH-α-MeDA+NAC (0.4mM +1mM), N-Me-α-MeDA (0.4 mM), or N-Me-α-MeDA+NAC (0.4mM +1mM) for 4 hrs. *$p<0.05$, ***$p<0.0005$ versus control. # $p<0.05$ versus treatment.